Figure S1

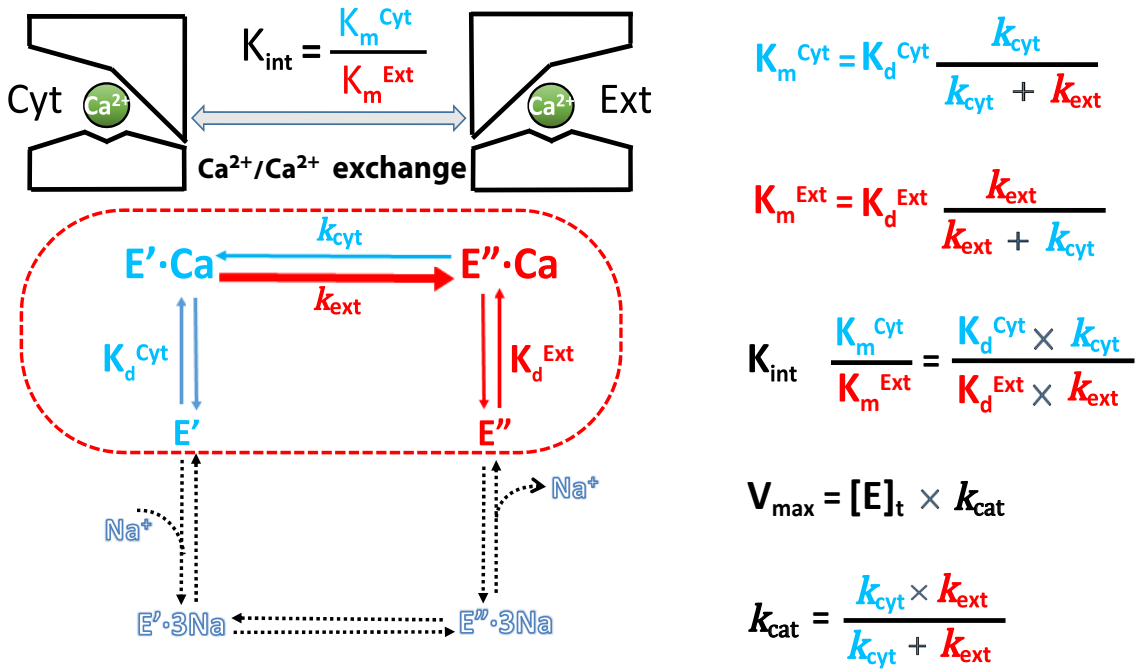

$$K_{int} = \frac{K_m^{Cyt}}{K_m^{Ext}}$$

$$K_m^{Cyt} = K_d^{Cyt} \frac{k_{cyt}}{k_{cyt} + k_{ext}}$$

$$K_m^{Ext} = K_d^{Ext} \frac{k_{ext}}{k_{ext} + k_{cyt}}$$

$$K_{int} \quad \frac{K_m^{Cyt}}{K_m^{Ext}} = \frac{K_d^{Cyt} \times k_{cyt}}{K_d^{Ext} \times k_{ext}}$$

$$V_{max} = [E]_t \times k_{cat}$$

$$k_{cat} = \frac{k_{cyt} \times k_{ext}}{k_{cyt} + k_{ext}}$$

Figure S1. The Ca^{2+}/Ca^{2+} exchange scheme. The present formalism is explored for evaluating the kinetic and equilibrium parameters of Ca^{2+}/Ca^{2+} exchange with a goal of quantifying the intrinsic equilibrium (K_{int}) and transport rates (k_{cat}) of bidirectional Ca^{2+} movements in different mutants. According to this formalism, the Ca^{2+} binding equilibrium constants (K_d^{Cyt} and K_d^{Ext}) and the rate constants of unidirectional Ca^{2+} transport (k_{cyt} and k_{ext}) account for the observed K_m^{Cyt} and K_m^{Ext} values. Taking into account the fact that NCX_Mj has very low turnover rates ($k_{cat} < 1 s^{-1}$) and high K_m^{Cyt} and K_m^{Ext} values (Figure S2) it is reasonable to assume that the transported $^{45}Ca^{2+}$ ions become effectively diluted in a huge pool of "unlabeled" Ca^{2+} inside the vesicles. Since the present experimental conditions satisfy the criteria of unidirectional Ca^{2+} movements, the present equations can be used for practical purposes. Namely, the intrinsic equilibrium of bidirectional Ca^{2+} movements ($K_{int} = K_m^{Cyt}/K_m^{Ext}$) can be presented as the ratio of the K_m^{Cyt} and K_m^{Ext} values. Thus, K_m^{Cyt} and K_m^{Ext} can be directly measured by detecting the unidirectional Ca^{2+} movements in two independent experiments. More specifically, K_m^{Cyt} can be determined at varying $[Ca]_{Cyt}$ and saturating $[Ca]_{Ext}$, whereas K_m^{Ext} can be measured at varying $[Ca]_{Ext}$ and saturating $[Ca]_{Cyt}$. Even though, the present formalism cannot distinguish between the equilibrium (K_d^{Cyt} and K_d^{Ext}) and kinetic (k_{cyt} and k_{ext}) "contributions" to the overall IF/OF equilibrium, K_{int} is still a very useful parameter for quantifying the functional asymmetry owned by a given mutant. In conjunction with this analysis, the transport rates (k_{cat}) can be derived from the $k_{cat} = V_{max}/[E]_t$ equation, by using the experimentally measured values of V_{max} and $[E]_t$ (see Materials and Methods).

Figure S2

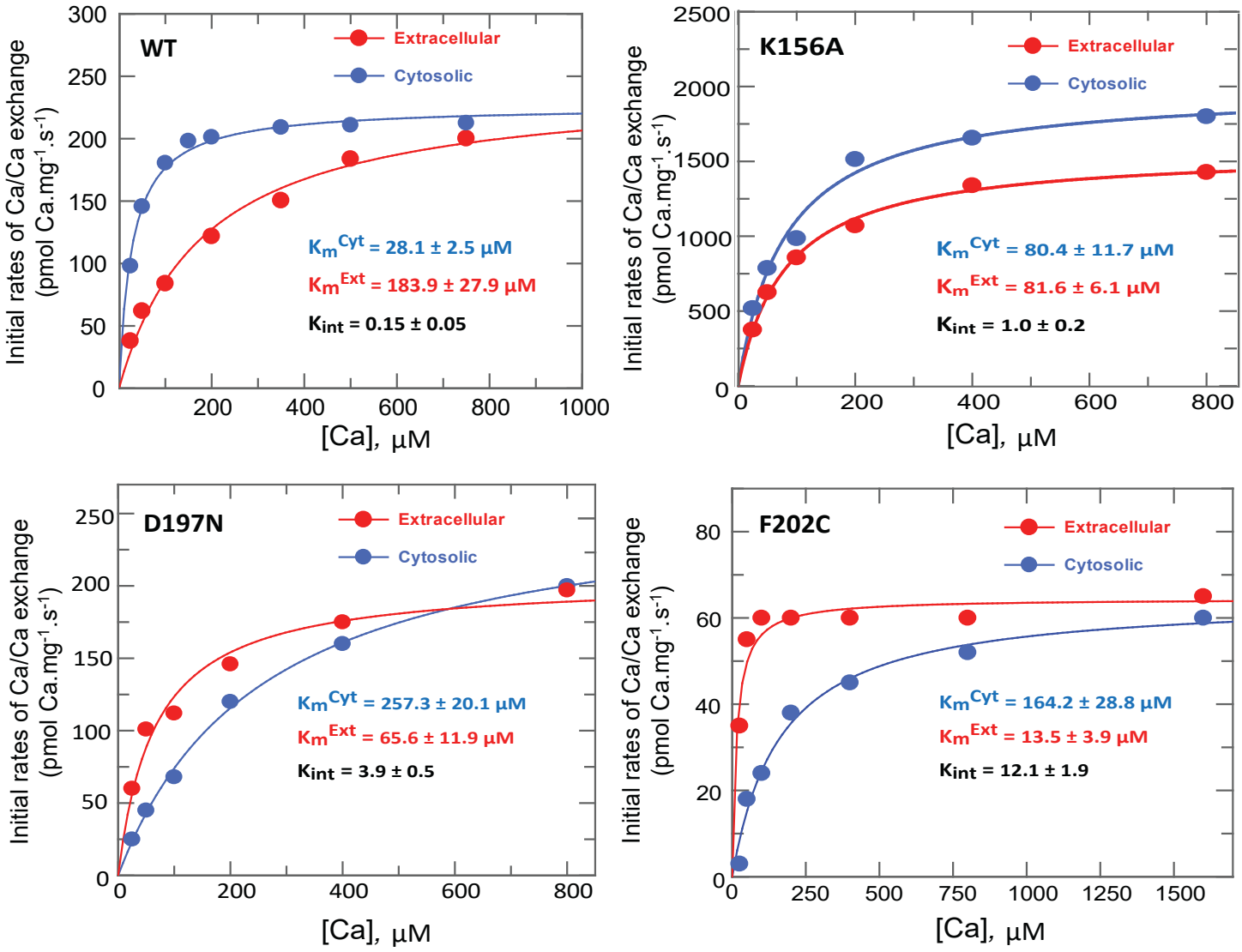

Figure S2. The K_m^{Cyt} and K_m^{Ext} values measured in three mutants. The initial rates of Ca^{2+}-dependent $^{45}Ca^{2+}$-uptake were measured for determining the K_m^{Cyt} and K_m^{Ext} values in three representative mutants (K156A, S197N and F202C). For this purpose, the E coli-derived vesicles containing a given mutant were preloaded with Ca^{2+} (as indicated below). The Ca^{2+}-loaded vesicles were diluted 200-500 fold in the assay medium containing $^{45}Ca^{2+}$ and the reaction of $^{45}Ca^{2+}$-uptake were quenched after 5 seconds by rapid injection of cold EGTA buffer (see Materials and Methods). The K_m^{Cyt} values were determined at varying $[Ca]_{Cyt}$ (2-1500 µM) and saturating $[Ca]_{Ext}$ (1500 µM), whereas the K_m^{Ext} values were measured at varying $[Ca]_{Ext}$ (2-1500 µM) and saturating $[Ca]_{Cyt}$ (1500 µM). The K_m and V_{max} values of the Ca^{2+}/Ca^{2+} exchange were obtained by fitting the experimental points with calculated lines by using a criteria of a minimal χ^2 value (GraFit 7.0 software, Erithacus Software, Ltd.). The standard errors (±SE) for K_m or V_{max} were calculated by using the matrix inversion method as recommended by GraFit 7

Figure S3

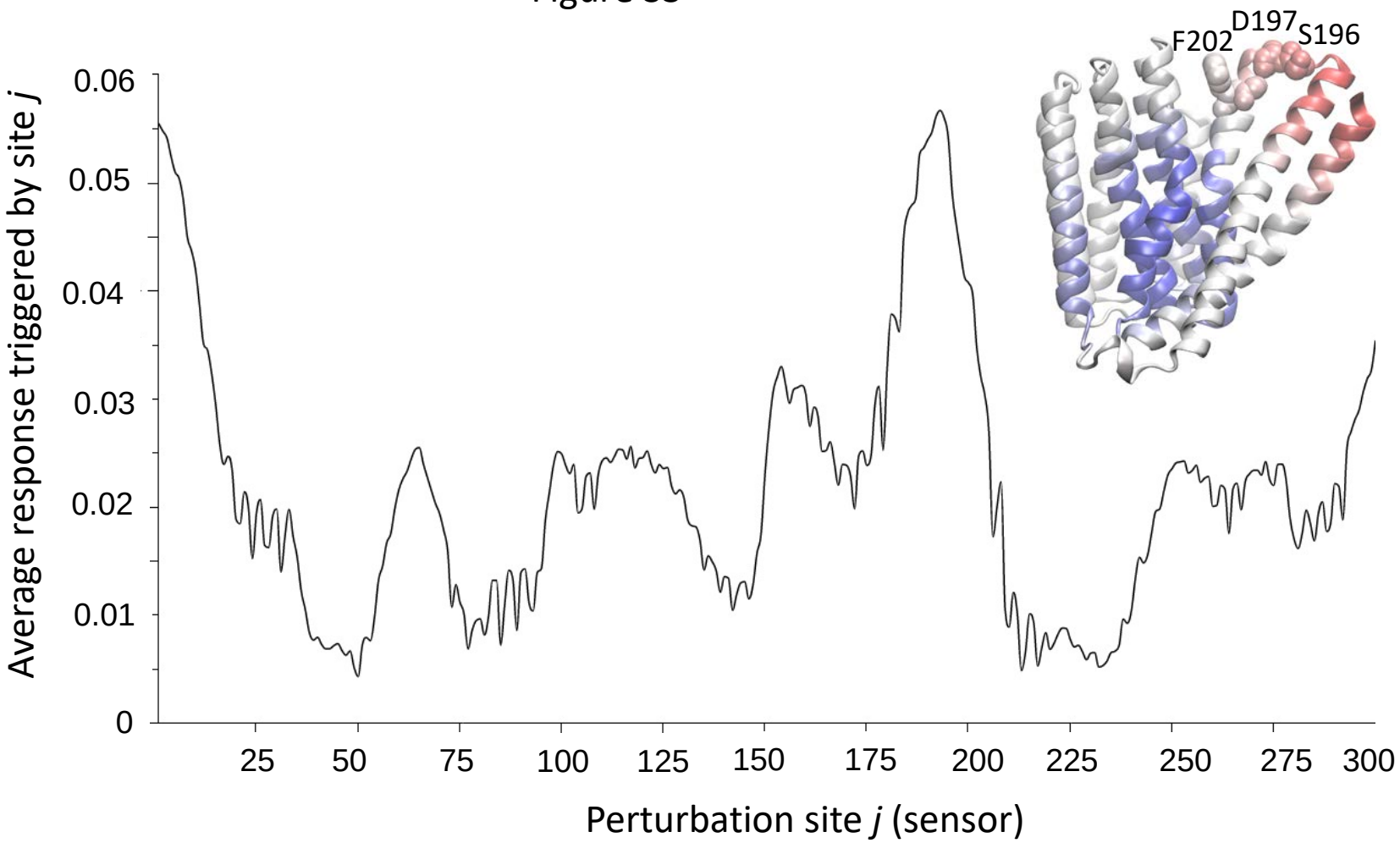

Figure S3: Propensity of NCX_Mj residues to serve as sensors, based on perturbation-response scanning (PRS) analysis. The PRS analysis identifies highly sensitive residues (peaks in the profile) that are likely to serve as sensors of allosteric signals. The inset protein structure is color-coded by the propensity to serve as sensors (red: most probable; blue: least probable). We note that the S196-D197-K198 segment in TM7 is distinguished by its high propensity for acting as a sensor in addition to the N-terminus.